Observations of zonal flow created by potential vorticity mixing in a rotating fluid

Julien Aubert, Sunghwan Jung, and Harry L. Swinney

Center for Nonlinear Dynamics and Department of Physics, The University of Texas at Austin, Austin, Texas, USA

[1]   We present an experimental and numerical study of a rotating fluid with a zonal flow produced from small-scale eddies, a common feature of many planetary systems. The apparatus consists of a water-filled annular tank with a sloped bottom. Flow is forced mechanically at small, non-axisymmetric scales. Potential vorticity is materially conserved and well-mixed. This implies the existence of nonzero axisymmetric vorticity and therefore of zonal flow, which has three zones in this case. The strength of zonal flow has an upper bound imposed by complete depletion of the beta-plane potential vorticity reservoir.   *INDEX TERMS:* 5707 Planetology: Fluid Planets: Atmospheres—structure and dynamics; 5734 Planetology: Fluid Planets: Magnetic fields and magnetism; 5744 Planetology: Fluid Planets: Orbital and rotational dynamics. **Citation:** Aubert, J., S. Jung, and H. L. Swinney, Observations of zonal flow created by potential vorticity mixing in a rotating fluid, *Geophys. Res. Lett.*, *29*(18), 1876, doi:10.1029/2002GL015422, 2002.

1.   Introduction

[2]   Fluid dynamics in many planetary systems is strongly influenced by the dominance of the Coriolis force over all other forces present in the system. A common feature of these systems is the generation of a zonal flow, i.e., a mean flow in the azimuthal direction with respect to the rotation vector. Zones of alternating azimuthal velocity have been observed on Saturn and Jupiter by Voyager spacecraft [*Ingersoll*, 1990]. The general circulation in the earth's atmosphere and oceans also displays azimuthal streams. Experiments [*Aubert et al.*, 2001] on convection in a rotating sphere of liquid metal modelling the earth's liquid core and numerical simulations [*Christensen*, 2001] show evidence of surface zonal flow generation from apparently chaotic, small scale deep convection plumes. A common feature of these systems is that mechanical or thermal forcing occurs at a scale which is small compared to the size of the system, and that zonal motion is therefore not directly forced.

[3]   In quasigeostrophic dynamics (see, e.g., *Pedlosky* [1987]), the beta-plane, a variation of the Coriolis force with latitude in the case of constant depth systems, or a variation of depth with radius in constant Coriolis force systems, plays an important role in the nonlinear mechanism of energy transfer to the zonal scale [*Rossby*, 1947; *Hide and James*, 1983]. The beta-plane can be seen as a reservoir of planetary vorticity. Potential vorticity (PV) can be defined as the sum of the planetary vorticity and the vorticity component parallel to the rotation vector in the rotating frame. In an inviscid fluid, PV is materially conserved and is therefore well-mixed in strongly forced environments. This leads to the development of zones of constant PV [*Rhines and Young*, 1982], and the resultant mean zonal shear leads to zonal flow.

[4]   Laboratory experiments [*Sommeria et al.*, 1989] and numerical simulations [*Marcus and Lee*, 1998] demonstrated that regions of constant PV existed within prograde and retrograde jets generated by forcing directly at the zonal scale. In those experiments, PV mixing, which is the process of geophysical interest, was not implied as a driving mechanism but as a consequence. Using the same rotating annulus system as *Sommeria et al.* [1991], in a different forcing configuration, we have conducted experiments and complementary numerical simulations where forcing occurs only at a small scale, and the strength and length scales of zonal flow are left unspecified and are selected by the dynamics.

[5]   Earlier experiments by *Colin de Verdière* [1979] and *McEwan et al.* [1980] on topographical and source-sink forced rotating flows demonstrated the role of Reynolds stresses in the generation of zonal circulation. In our study both experimental and numerical imaging support an equivalent interpretation in terms of PV mixing. This allows us to show in addition that the magnitude of zonal flow has an upper bound determined by the quantity of PV available in the planetary reservoir. The evolution of the flow towards its perfect mixing limit is studied as a function of the two control parameters of the experiment, rotation rate and pumping rate.

2.   Model

[6]   The experimental set-up is a water-filled annular tank of inner radius $r_i = 10.8$ cm and outer radius $r_0 = 43.2$ cm. The tank is covered by a solid transparent lid. It can be spun up to rotation frequencies $\Omega/2\pi$ of 3 Hz. The bottom depth varies from 17.1 cm at the inner radius to 20.3 cm at the outer radius, with a mean height $h_0 = 18.7$ cm and a slope $\eta = -0.1$. Water is continuously pumped in closed circuit in and out of the tank, through a ring of 120 circular holes located at the bottom of the tank at $r_f = 27.0$ cm, halfway between the annulus boundaries. Holes in a semi-circle (see Figure 1) are sources, and holes in the opposite semi-circle are sinks. Each hole has a diameter of 0.25 cm, and the total pumping rate F is in the range $50-550$ cm^3/s. Above each source (sink) the vertical flow creates a local divergence (convergence) which, in less than one tank turn, is converted by the Coriolis force into an anticyclone (cyclone). Small scale forcing of the flow is achieved in this way. Since the net vorticity produced is zero, zonal flow is not directly forced. This system is therefore a convenient approximation of the examples described in the introduction.
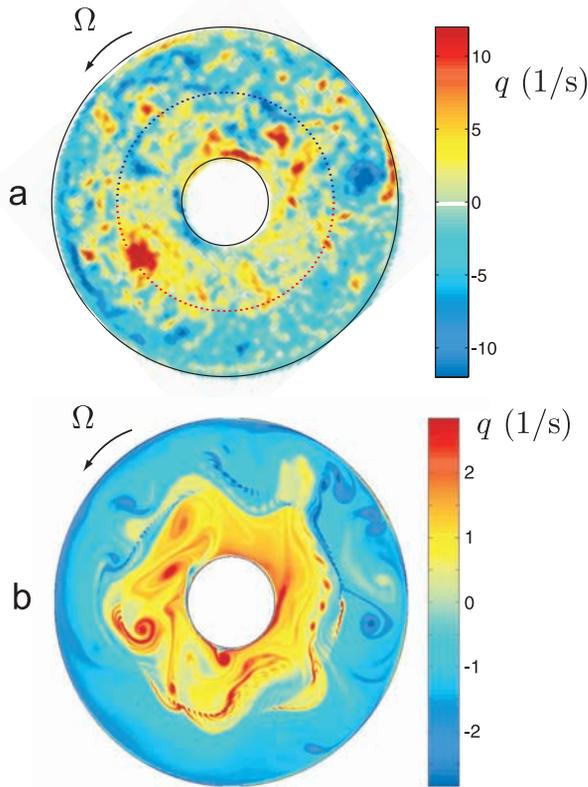
Figure 1. The potential vorticity fields obtained from (a) experiment, and (b) numerical simulation contain strong cyclones (red) and anticyclones (blue). Image (a) shows the location of the forcing holes, arranged in semi-circles of 60 sources (blue) and 60 sinks (red); the same forcing was used in the simulations. This forcing produces vortex filaments of the same width as holes (see striations in b); the filaments merge and mix potential vorticity in the inner and outer regions of the annulus, and a retrograde drifting Rossby wave (visible particularly in b) prevents mixing between the two regions. In (a), rotation rate $\Omega/2\pi$ = 2.5 Hz and pumping rate F = 550 cm^3/s (Reynolds number, 20000); in (b), $\Omega/2\pi$ = 1.5 Hz and F = 75 cm^3/s. Numerical simulations with stronger forcing than in b exhibit behavior similar to a, with more small scale vortices than b.

[7] The Rossby number $Ro = (\tau_\omega \Omega)^{-1}$ is defined using the nonzonal vortex turnover time

$$\tau_\omega = \left(\frac{1}{\pi(r_o^2 - r_i^2)} \int_{ri}^{ro} \int_0^{2\pi} \overline{r(\omega - \overline{\omega_\theta})_t^2} \, dr d\theta \right)^{-1/2} \quad (1)$$

where ω is the vorticity component parallel to the rotation axis, $\overline{\omega_t}$ its time-average and $\overline{\omega_\theta}$ its azimuthal average. Ro is kept under 0.2 to maintain quasigeostrophy and a flow reasonably two-dimensional by the Taylor-Proudman theorem.

[8] In the experiment, Particle Image Velocimetry was used to determine the complete velocity field in a plane perpendicular to the axis of rotation [*Baroud et al.*, 2002]. A horizontal light sheet was produced using a ring of light emitting diodes at mid-depth of the tank. Water in the tank

was seeded with neutrally buoyant plastic particles of size ~0.1 mm. For each pair of values for the control parameters Ω and F, 100 instantaneous velocity fields were acquired at intervals of about 1, 2, 4 or 8 seconds for forcings of 550, 350, 150 and 50 cm^3/s, respectively.

[9] Direct two-dimensional numerical simulations have been performed in addition to the experiments. We resolved the advection-diffusion of PV including viscous dissipation (viscosity ν), realistic forcing, and drag characterized by the Ekman spin-up time τ_E:

$$\frac{\partial q}{\partial t} + (\mathbf{u} \cdot \nabla)q + \frac{\omega}{\tau_E} = \nu\nabla^2\omega + \frac{2\Omega}{h_0} v_f, \quad (2)$$

$$\tau_E = \frac{h_0}{2}(\nu\Omega)^{-1/2}, \quad (3)$$

where the vertical velocity at each forcing hole is described by v_f, which was chosen to be constant over each hole and zero elsewhere. Equation (2) was solved on an annulus of the same aspect ratio as the experiment, with rigid boundary conditions at the inner and outer radii. The numerical technique was finite-differencing in the radial direction and spectral decomposition in the zonal direction. Each forcing hole typically spanned ten mesh points.

3. Results

[10] The potential vorticity is given by $q = \omega + \beta(r - r_f)$, where r is the radial coordinate, and the beta-plane parameter is $\beta = 2\eta\Omega/h_0$. A snapshot of the measured q is shown in Figure 1a. We observe that one large anticyclone (cyclone) appears intermittently in the source (sink) half of the annulus. Both drift in the retrograde direction with respect to the annulus. The strongly forced flow is dominated by vortices so no zonal pattern is apparent in snapshots; however, time averaging clearly reveals a zonal flow pattern, as Figure 2 illustrates. A PV gradient exists above the forcing ring, while PV is well mixed (roughly uniform) in the inner region ($r_i < r < r_f$) and in the outer region ($r_f < r < r_o$). Graphs of the azimuthally averaged PV (Figure 2b) and the azimuthal velocity (Figure 2c) as a function of r show that the forcing has created three zones for azimuthal flow: the PV gradient region corresponds to a prograde zonal circulation, while the regions of approximately constant PV correspond to retrograde zonal circulations. The prograde flow has a profile consistent with sech$^2(r)$ (Figure 2c), as previously observed by *Sommeria et al.* [1989]. This is a popular model for jets in rotating experiments because it allows mathematically tractable marginal stability calculations. The retrograde flow is weaker in the outer region. This three-zone flow structure was observed for all parameter values F and Ω studied.

[11] The numerical simulation shows that small scale PV filaments are released above each hole in the forcing ring (Figure 1b), and positive (negative) filaments merge into cyclonic (anticyclonic) structures. The beta plane acts as a vorticity selector: cyclonic (anticyclonic) structures cannot move outwards (inwards) because their motion outwards (inwards) triggers a Rossby wave which restores them to their original position. In contrast, nothing prevents a cyclone from moving to the inside. In this way, positive
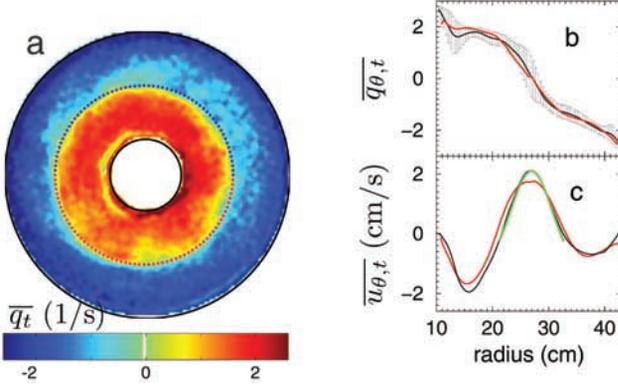
Figure 2. The experimental time-averaged potential vorticity field $\overline{q_t}$ (a) and azimuthally-averaged profile $\overline{q_{\theta,t}}$ (b, black line) have a positive (negative) roughly uniform value in the inner (outer) region of the annulus. Numerical simulations (b−c, red lines) yield a similar profile. (c) The average azimuthal velocity profile $\overline{u_{\theta,t}}$ is consistent with profile (b) and Stokes theorem (see text) and reveals three zonal flows, retrograde in the regions of well-mixed potential vorticity and prograde in the gradient region. The vicinity of the peak of zonal flow is described by $sech^2(r)$ (green line in c). Conditions for experiment and simulation were $\Omega/2\pi = 2.5$ Hz and $F = 150$ cm^3/s.

(negative) PV is carried by cyclones (anticyclones) to the the inner (outer) region of the annulus. A gradient therefore sets up above the forcing ring, separating the two regions where vortical structures mix PV into two homogeneized, constant levels. A retrograde-drifting Rossby wave, similar to that observed by *Sommeria et al.* [1991], rides on the PV gradient, preventing the inner and outer regions from exchanging fluid most of the time, although there are a few leaks across the PV gradient, as can be seen in Figure 1b.

[12] The net vorticity injected by the forcing system is zero (cyclonic and anticyclonic vorticity are injected in balance); hence material conservation of PV implies that the only PV to be homogeneized is the planetary background $\beta(r - r_f)$. In the limit of perfect mixing, the PV has two levels, q_i in the inner region and q_o in the outer region, and these levels are given by the mean values of the planetary background in each region,

$$q_{i,o} = \frac{2\pi}{\pi\left(r_f^2 - r_{i,0}^2\right)} \int_{r_{i,o}}^{r_f} r\,\beta(r - r_f)dr = \frac{\beta}{3}\left(-r_f + \frac{2r_{i,o}^2}{r_f + r_{i,o}}\right)$$

(4)

which are independent of the forcing strength.

[13] In the limit of strong mixing, the homogenized PV levels scale linearly with β. In Figure 3 the experimental radial PV profiles are normalized by β. They become fairly independent of forcing rate and rotation rate. In contrast to the perfect mixing model, which has an infinite gradient above the forcing ring, a finite gradient zone remains in the experimental data, of width l approximately one fourth of the annular channel width. Although sharp radial PV gradients exist locally in the vicinity of the forcing ring,

as Figure 1b illustrates, zonal averaging as in Figure 3 smooths them. For a jet with a sech^2 profile, the modenumber m of the Rossby wave riding on the steep PV gradient is predicted by marginal stability analysis (see *Sommeria et al.* [1989] and references therein) to be $m = 2^{1/2}l^{-1}r_f$. The value $m = 5$ observed in our numerical simulations at low forcing level (Figure 1b) agrees with this prediction.

[14] The mean zonal flow $\overline{u_\theta}$ is related to azimuthally averaged vorticity $\overline{\omega_\theta}$ through Stokes theorem

$$\overline{u_\theta}(r) = \frac{1}{r}\int_{r_i}^{r} r\overline{\omega_\theta}dr = \frac{1}{r}\int_{r_i}^{r} r\left(\overline{q_\theta} - \beta(r - r_f)\right)dr. \quad (5)$$

Equation (5) shows that zonal shear, and therefore zonal motion, exists as a consequence of PV mixing by smaller scale eddies. A perfectly mixed zonal flow will have the same properties as perfectly mixed PV, i.e., it will be proportional to β and independent of forcing. It will also have a cusp at $r = r_f$ (due to the discontinuity in the PV profile), and will be always retrograde and of equal strength in the inner and outer regions. The cusp is not observed in our moderately forced flows. A prograde region exists because flow near boundaries does not conserve PV and injects some into the fluid (see Figure 1b). The zonal flow is asymmetric with respect to r_f because the inner region is smaller and therefore better mixed than the outer region (see distribution of vortices in Figure 1b).

[15] Any dependence of the observed zonal flow on the forcing strength is due to incomplete PV mixing. The mixing is nearly complete, as illustrated by Figure 4, where the rms value U_θ of the measured time-averaged zonal motion is normalized with respect to its perfect mixing value, obtained from equations (4) and (5):

$$U_\infty = \beta\delta^2\sqrt{\frac{2}{15}} \approx \frac{\beta\delta^2}{3}, \quad (6)$$

where the curvature of the annulus has been neglected, and δ = $(r_o − r_i)/4$ is a length representative of the width of constant PV zones. U_θ/U_∞ is plotted in Figure 4 as a function of the ratio of time scales τ_E/τ_ω, which measures the importance of nonzonal motion, which favors mixing,
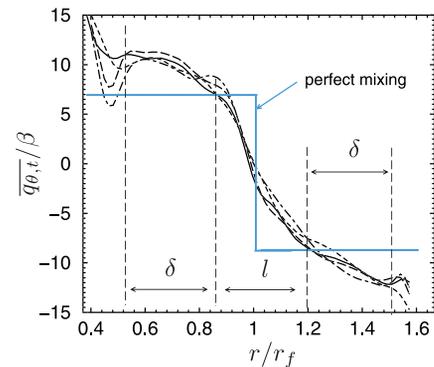

Figure 3. The observed well-mixed profiles of potential vorticity are similar when normalized by the beta plane coefficient β. Lengths δ and l of the mixing and gradient regions are then determined solely by the geometry. The values of $\Omega/2\pi$ (Hz) and F (cm^3/s) were 1.25, 150 (−); 2.5, 150 (− −); 2.5, 350 (− −); 2.5, 550 (− − −).
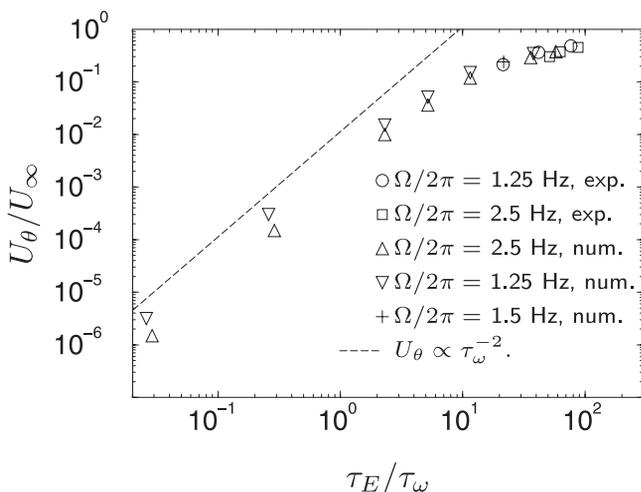
Figure 4. The forcing configuration has zero net potential vorticity injection, and the planetary reservoir has a limited capacity: The rms value U_θ of zonal flow approaches an upper bound U_∞ when mixing, measured by the ratio of Ekman spin-up time τ_E to vortex turnover time τ_ω, becomes large.

relative to the friction (in the top and bottom Ekman layers), which inhibits mixing. The experiments, conducted mainly in the well-mixed regime ($\tau_E/\tau_\omega \gg 1$), and the numerical simulations are in reasonable agreement in the region of overlap. In the viscous regime ($\tau_E/\tau_\omega \ll 1$), zonal motion grows with the square of the radial component of flow, hence with τ_ω^{-2}, reflecting the action of the zonal component of Reynolds stresses [*McEwan et al.*, 1980]. In the well-mixed regime, the zonal motion clearly saturates and never exceeds the perfect mixing value. In this limit, the planetary reservoir is depleted and there is no way the system can put more energy into zonal flow. In the experiments, perfect mixing will never be reached due to the Rossby wave instability and nonconservation of PV near boundaries of the annulus.

4. Discussion

[16] These experiments illustrate how non-axisymmetric motion mixes PV and produces a zonal circulation. As the PV mixing grows, a state is reached where the reservoir of planetary vorticity is fully used, and the zonal motion saturates at an rms value given by Equation (6), as Figure 4 illustrates. Saturation of zonal flow has been observed in the three-dimensional numerical simulations of *Christensen* [2001], and has been attributed to a loss of two-dimensionality in the system as the Rossby number grows. Here we show that a two-dimensional model also produces saturation.

[17] The criterion for saturation may be written in terms of nondimensional numbers, namely the Rossby number $Ro = U/\Omega D$ and the Ekman number $E = (\tau_E \Omega)^{-2} = \nu/\Omega D^2$, where D is a typical length scale for the system and U a typical nonzonal velocity:

$$Ro E^{-1/2} \gg 1. \qquad (7)$$

With this condition satisfied, relation (6) may be expected to hold quite generally, since it only expresses that $\overline{\omega}$ is

bounded. Approximating the atmosphere of Jupiter with a well-mixed, piece-wise constant PV, such as done by *Marcus* [1993], one can thus relate the typical zonal velocity to the size of the zones. We obtain the correct order of magnitude for the zonal velocity, $U_\infty = 50$ m/s, using the following values: $\delta = 2000$ km for the width of a zone; $\beta = 2\Omega \cos \theta/r$, where θ is the latitude; $\Omega = 1.75 \times 10^{-4}$ rad/s; $\theta = \pi/4$; and $r = 71400$ km.

[18] In the flow in an annulus that we have studied, even though the characteristics of zonal flow are not specified by the forcing, the system evolves towards a state with fixed number of zones whose strength and length scale are prescribed by the geometry. The question of how many zones a random small-scale mechanical or thermal forcing would produce remains open and will be examined in forthcoming experimental studies.

References

Aubert, J., D. Brito, P. Cardin, H.-C. Nataf, and J.-P. Masson, A systematic experimental study of spherical shell rotating convection in water and liquid gallium, *Phys. Earth Planet. Int.*, *128*, 51–74, 2001.

Baroud, C. N., B. B. Plapp, Z.-S. She, and H. L. Swinney, Anomalous self-similarity in a turbulent rapidly rotating fluid, *Phys. Rev. Lett.*, *88*, 114501-1–114501-4, 2002.

Christensen, U. R., Zonal flow driven by deep convection in the major planets, *Geophys. Res. Lett.*, *13*, 2553–2556, 2001.

Colin de Verdière, A., Mean flow generation by topographic Rossby waves, *J. Fluid Mech.*, *94*, 39–64, 1979.

Hide, R., and I. N. James, Differential rotation produced by potential vorticity mixing in a rapidly rotating fluid., *Geophys. J.R. Astr. Soc.*, *74*, 301–312, 1983.

Ingersoll, A., Atmospheric dynamics of the outer planets, *Science*, *248*, 308–315, 1990.

Jault, D., C. Gire, and J. L. Le Moul, Westward drift, core motions and exchanges of angular momentum between core and mantle, *Nature*, *333*, 353–356, 1988.

Marcus, P. S., Jupiter's great red spot and other vortices, *Annu. Rev. Astron. Astrophys.*, *431*, 523, 1993.

Marcus, P. S., and C. Lee, A model for eastward and westward jets in laboratory experiments and planetary atmospheres, *Phys. Fluids*, *10*, 1474–1489, 1998.

McEwan, A. D., R. O. R. Y. Thompson, and R. A. Plumb, Mean flows driven by weak eddies in rotating systems, *J. Fluid Mech.*, *99*, 655–672, 1980.

Pedlosky, J., *Geophysical fluid dynamics*, Springer, New-York, 1987.

Rhines, P. B., and W. R. Young, Homogenization of potential vorticity in planetary gyres, *J. Fluid Mech.*, *122*, 347–367, 1982.

Rossby, C., On the distribution of angular velocity in gaseous envelopes under the influence of large-scale horizontal mixing process, *Bull. Am. Met. Soc.*, *28*, 53–68, 1947.

Sommeria, J., S. D. Meyers, and H. L. Swinney, Laboratory model of a planetary eastward jet, *Nature*, *337*, 58–61, 1989.

Sommeria, J., S. D. Meyers, and H. L. Swinney, Experiments on vortices and Rossby waves in eastward and westward jets, in *Nonlinear Topics in Ocean Physics*, edited by A. Osborne, p. 227, North-Holland, Amsterdam, 1991.

———————————
J. Aubert, Institut für Geophysik, Universität Göttingen, Herzberger Landstrasse 180, 37075 Göttingen, Germany. (jaubert@uni-geophys. gwdg.de)

S. Jung and H. L. Swinney, Center for Nonlinear Dynamics and Department of Physics, The University of Texas at Austin, Austin, Texas 78712, USA. (swinney@chaos.ph.utexas.edu)